Numerical Modeling of Space Plasma Flows: ASTRONUM-2011
ASP Conference Series, Vol. 459
N. V. Pogorelov, J. A. Font, E. Audit, and G. P. Zank, eds.

3D MHD Numerical Study of Two CMEs' Evolution and Their Interaction

Fang Shen,[1,2] Xueshang Feng,[1] and S. T. Wu[2]

[1]*SIGMA Weather Group, State Key Laboratory of Space Weather, Center for Space Science and Applied Research, Chinese Academy of Sciences, Beijing 100190, China*

[2]*Center for Space Plasma and Aeronomic Research, The University of Alabama in Huntsville, Huntsville, AL 35899 USA*

Abstract. To modeling the propagation and interaction of two CMEs, the three-dimensional (3D) time-dependent, numerical magnetohydrodynamic (MHD) model is applied. With help of the observation data of magnetic field and density, the background solar wind is constructed based on the self-consistent source surface. By means of the magnetized plasma blob model, two successive CMEs occurring on 2001 March 28 and forming a multiple magnetic cloud (multi-MC) in interplanetary space is simulated. The dynamical propagation and interaction of the two CMEs are investigated. We have found that, the second CME can overtake the first one, and cause compound interactions and an obvious acceleration of the shock. At L1 point near the Earth, the two resultant magnetic clouds in our simulation are consistent with the observations by ACE.

1. Introduction

It is well-known that coronal mass ejections (CMEs) and their interplanetary consequences (ICMEs) represent different aspects of the same phenomenon responsible for large non-recurrent geomagnetic storms. It is very important to understand the propagation of CMEs in the corona and their physical relationship to ejecta propagating through the interplanetary medium (Wu et al., 1999). It is believed that successive ICMEs can merge with each other and form a compound structure, with the improvement of coronagraphic observations and the presence of the solar wind measurement in the outer heliosphere (Voyager, Ulysses), as mentioned formerly (e.g., Burlaga et al., 2002 and Lugaz et al., 2011). The same phenomenon also happens in the inner heliosphere, before CMEs reach Earth. When two or more ejections interact, they can form the well-known multiple ICME or magnetic cloud structure (Wang et al., 2003). These CMEs interactions result in different solar wind signatures as well as different geoeffectiveness as compared to isolated CME events.

The event of multiple magnetic clouds (Multi-MC) in interplanetary space on March 31, 2001, causing the largest geomagnetic storm with Dst = -387 nT during the 23th solar maximum (2000-2001), was studied by many authors (Wang et al., 2003, 2005; Lugaz et al., 2005). In those studies for this event (eg. Wang et al., 2005), the bimodal solar wind model was used for the background solar wind, and the two CMEs were assumed to propagate in the same direction. A bimodal solar wind model may be

suitable to reflect solar minimum conditions but this CMEs interaction event occurred near solar maximum. Moreover, SOHO/EIT observations showed that the two halo CMEs forming the Multi-MC event originated from the solar surface source regions around N20E22 and N18E02 on 2001 March 28 (Wang et al., 2003), which means that the two CMEs did not propagate along the same direction. Thus, this two CMEs interaction event should be better treated as an oblique collision than a direct collision. Their result implied that the travel time of a MultiMC structure was almost determined by the preceding slow cloud but they cannot simulate the associated shock.

In the present paper, we employ a 3D MHD code (COIN-TVD MHD model) with self-consistent source surface structures as initial-boundary conditions (Shen et al., 2007, 2011a, 2011b), which is derived from the observation of the solar magnetic field and K-coronal brightness. The high-density, -velocity and -temperature magnetized plasma blob model (Chané et al. 2005, 2006, 2008; Shen et al., 2011a, 2011b) is used for the launching of the two halo CMEs observed by SOHO/LASCO on 2001 March 28. According to the observation, the center of the two blobs is located at N20E22 and N18E02, respectively. The simulated background solar wind is presented in §2, the simulation of the propagation and interaction of the 2001 March 31 two CMEs event is given in §3. Finally a summary is given in §4.

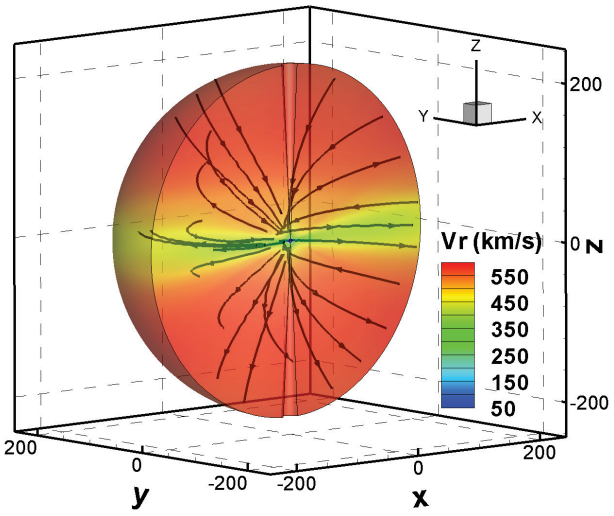

Figure 1. The calculated steady-state 3D magnetic field lines and radial velocity distribution, from 2.5 Rs to 220 Rs at 100 hours (Unit of the axis: Rs)

2. 3D MHD Simulation of Solar Wind Background for CR 1974

The numerical 3D MHD scheme used in the COIN-TVD MHD model is a modified Total Variation Diminishing /Lax-Friedrichs (TVD/LF) type scheme (Feng et al., 2005; Shen et al., 2007, 2011a, 2011b) with electric field modification method (Tóth, 2000) for the assurance of $\nabla \cdot \vec{B} = 0$. The time-dependent 3D ideal MHD equations also include solar rotation and volumetric heating. The equations can be written in a spherical-

component form at the inertial (non-rotating) reference frame, which was described in detail in our pervious paper (Shen et al., 2007).

The self-consistent source surface distribution is used as the initial-boundary conditions at 2.5 Rs (Wei et al., 2003; Shen et al., 2007, 2010, 2011a, 2011b), based on the the photospheric magnetic observation and the K coronal polarized brightness (pB). The detailed description is given in Shen et al. (2011b) which will not be repeated here. In order to reasonably accommodate the source surface distribution into our MHD model, the method of projected characteristics (Wu and Wang, 1987; Wu et al., 2006; Shen et al., 2011a, 2011b) is employed at the lower boundary (2.5 Rs). At the outer boundary of 220 Rs, we employ a linear extrapolation.

To save computation time and maintain simulation accuracy, we use the asynchronous and parallel time-marching method by using different local time steps (adapted to the local CFL condition) in the corona (2.5 Rs to 22 Rs) and the heliosphere (22 Rs to 220 Rs), and applying parallel computation in the r-direction for this simulation (Shen et al., 2009). The calculated steady-state 3D magnetic field topology and radial velocity distribution are shown in Figure 1. It takes $\sim$ 100 hours to reach the MHD equilibrium state. The well-known Archimedes' spiral lines are reproduced in Figure 1.

3. Numerical Simulation of 2001 March 28-31 two CMEs Event

3.1. CME Launching

Detailed descriptions of the 2001 March 28 event have been reported by Wang et al. (2003). For completeness we will summarize some of the highlights for this event.

The first halo CME was visible in LASCO/C2 at 01:27 UT on 28 March 2001, located at N20E22. The projected speed according to the LASCO CME catalog is 427 km/s. The second halo CME was visible in C2 at 12:50 UT on the same day, located at N18E02. The projected speed is 519 km/s according to the LASCO CME catalog. On 2001 March 31, a very intense forward shock arrived at the L1 point (1.5×10^9m from the Earth to sunward) at 00:20 UT based on the ACE spacecraft observation. Then, the first magnetic cloud was observed from 0505 UT to 1015 UT and the second one was observed during 1235 UT - 2140 UT. This Multi-MC event caused the largest geomagnetic storm with Dst value of -387 nT during the 23th solar maximum (2000-2001) (Wang et al., 2003).

To simulate this two-CME event, two magnetized plasma blobs are superimposed successively on a background steady state solar wind medium and a disturbed solar wind medium, respectively. The magnetized plasma blob model given by Chané (2005, 2006, 2008) is a kind of very simple non force free flux rope model for CME launching, which has relative simple type and can reproduce some features about the magnetic cloud. The density, radial velocity and temperature profiles of the initial perturbation are defined as follows:

$$V_{\rm cme} = \frac{v_{\rm max}}{2}\left(1-\cos\pi\frac{a_{\rm cme}-a}{a_{\rm cme}}\right), \quad (1)$$

$$\rho_{\rm cme} = \frac{\rho_{\rm max}}{2}\left(1-\cos\pi\frac{a_{\rm cme}-a}{a_{\rm cme}}\right), \quad (2)$$

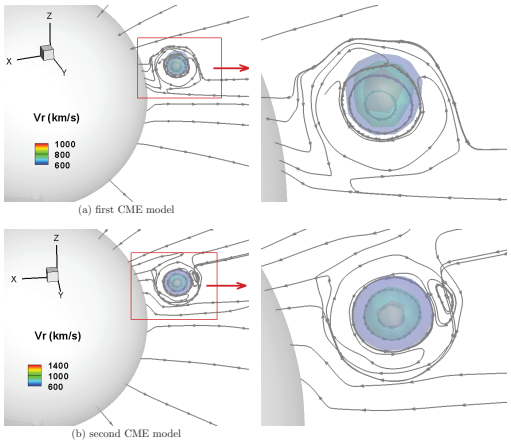

Figure 2. The three-dimensional views of the isosurface of the radial velocity v_r and the initial magnetic field lines of the CME initialization for CME1 (a) and CME2 (b), including zooming in on the plasma blob.

$$T_{\rm cme} = \frac{T_{\rm max}}{2}\left(1-\cos\pi\frac{a_{\rm cme}-a}{a_{\rm cme}}\right), \tag{3}$$

where $a_{\rm cme}$ is the radius of the initial plasma blob, a denotes the distance from the center of the initial plasma blob, and $\rho_{\rm max}$, $V_{\rm max}$ and $T_{\rm max}$ are the maximum density, radial velocity and temperature in the plasma bubble added on top of the background solar wind, respectively.

The initial magnetic field of the perturbation in r and θ direction can be defined as (Shen et al., 2011a, 2011b)

$$B_{r_{\rm cme}} = -\frac{1}{r^2\sin\theta}\frac{\partial\psi}{\partial\theta},\ B_{\theta_{\rm cme}} = \frac{1}{r\sin\theta}\frac{\partial\psi}{\partial r} \tag{4}$$

where

$$\psi = \psi_0\left[a-\frac{a_{\rm cme}}{2\pi}\sin\left(\frac{2\pi a}{a_{\rm cme}}\right)\right] \tag{5}$$

is the magnetic flux function.

In our simulation, the radius of the two plasma blobs $a_{\rm cme}$ is set as 0.5 Rs and the center of the initial plasma blobs is situated at 3.5 Rs. The second plasma blob is initiated 10 hrs after the launch of the first one. The other parameters are given in TABLE 1.

TABLE 1

	The first CME (CME1)	The second CME (CME2)
$\theta_{\rm cme}$	20°	18°
$\varphi_{\rm cme}$	158°	178°
$\rho_{\rm max}(\rm cm^{-3})$	1.2×10^9	1.5×10^9
$v_{\rm max}$(km/s)	1200	1500
ψ_0	2.0	−2.4

The two panels of Figure 2 display the 3D intuitive views of the isosurfaces with three values of the radial velocity v_r and the initial magnetic field lines of CME1 (a)

and CME2 (b) initialization on the background solar wind, including zooming in on the plasma blob. Figure 2(a) and 2(b) show that the maximum value of the radial velocity appeared at the center of the initial plasma blob in the two CMEs initialization, and the magnetic field of CME2 has initially the inverse polarity compared with CME1.

3.2. The Dynamical Propagation and Interaction of the two CMEs, and the Properties at L1 Point

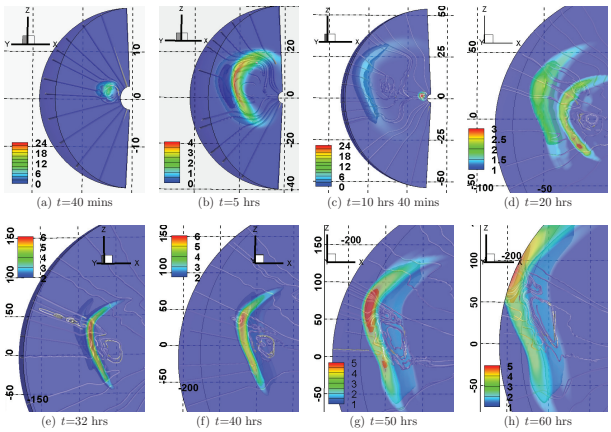

Figure 3. A Three-dimensional representation of the CMEs shown 40 minutes (a), 5 hours (b), 10 hours 40 minutes (40 minutes after the second CME launched) (c), 20 hours (d), 32 hours (e), 40 hours (f), 50 hours (g) and 60 hours (h) after the first CME launching. The solid rod-shaped lines are magnetic field lines, and the color codes represent the relative density $((\rho - \rho_0)/\rho_0)$) (Unit of the axis: Rs).

In this section, the simulation results are presented. Figure 3 show the 3D propagation of the simulated CMEs at eight consecutive times after the launch of CME1. The shock fronts with a high relatively high density are clearly visible in Figures 3. At time t=40 minutes, the flux rope of CME1 still remain an almost circular shape, but is quickly stretched to a pancake shape after t=5 hours. At t=20 hours, the two flux ropes get closer. At t = 32 hours, the shock front of CME2 reaches the trailing edge of CME1. Then from 32 - 40 hours, the shock of CME2 penetrates through the body of CME1. From time t = 40 hours, the two shocks begin to merge to a stronger combined shock, seen from panels (e), (f) of Figure 3. In panels (e)-(h) of Figure 3, after time t = 32 hours, the flux rope of CME2 with relative low density overtakes the flux rope of CME1, and the oblique collision occurs between the two flux ropes. It induces obvious deformation and compression of the two flux ropes.

Figure 4 shows the comparison of the computed plasma and field parameters at L1 point in the right column with the observed Multi-MC of 2001 March 31 - April 1 shown in the left column. At L1 point, the two flux ropes have evolved to show some of the characteristics commonly associated with Multi-MC, namely two high magnetic field strength regions separated by a region of increased β, smooth variation of the magnetic field in each cloud, a shorter duration of the first cloud compare to the second one, low proton density and temperature in both clouds and a high velocity profile (Wang et al., 2003; Lugaz et al., 2005). As seen in the column (b) of Figure 4, the

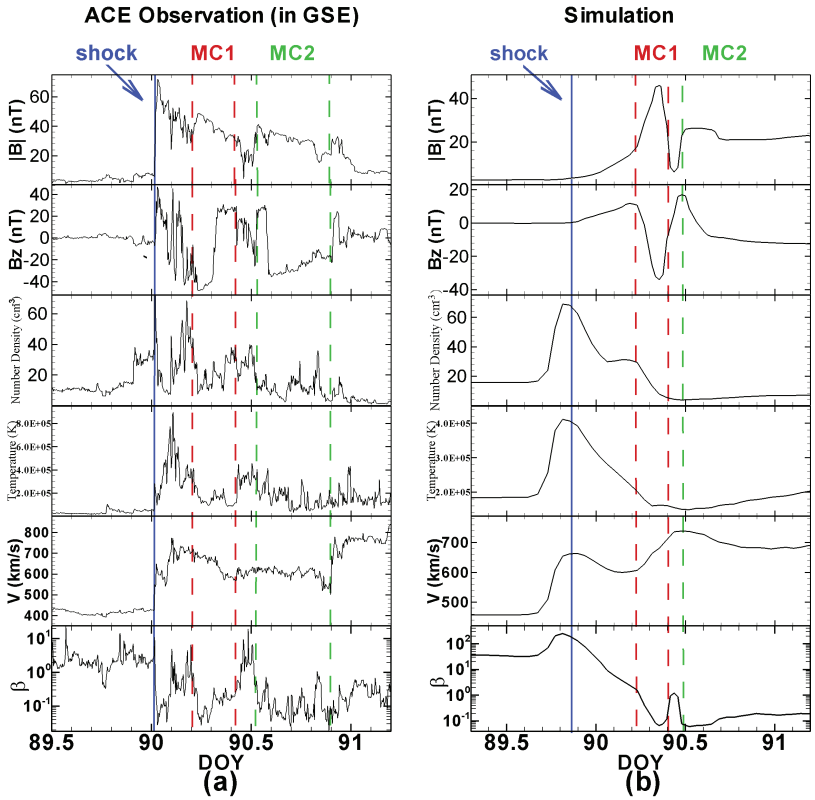

Figure 4. A comparison of the MHD simulation of the magnetic field and plasma parameters with the measured (ACE spacecraft) magnetic field and solar wind parameters at L1 point in 2001. The left column (column (a)) and the right column (column (b)) denote the measured parameters by ACE and simulation parameters, respectively, (top to bottom) the magnetic field strength $|B|$ (nT), B_z (nT) at GSE coordinate system, the proton density (cm^{-3}), the plasma temperature (K), the velocity (km/s) and the plasma β.

simulated shock reaches L1 at DOY of 89.86, marked with the blue vertical solid line, and the two magnetic clouds are preceded by a very strong shock with high density, temperature and velocity.

Comparing our simulation result with ACE data, we find that in spite of the simple CME model used, our simulation is in good qualitative agreement with the data. The two MCs are preceded by a very strong shock with high density, temperature and velocity. For the z-component of the magnetic field, the simulated and measured profiles at the L1 point are similar, becoming northward first, then changing to southward, later changing to northward again, and finally turning southward. And the southward component of the magnetic field reaches a maximum value in MC1 and remains southward for a long time, which lead to a peak value of Dst of -387 nT (Wang et al. 2003).

Some quantitative disagreement between our simulation and reality is to be expected. The shock center characterized by the maximum value of the velocity arrives earlier in the simulation. The maximum value of the magnetic filed strength and tem-

perature in the simulation is much smaller than that in the ACE data, respectively. We believe that more solar and interplanetary observations will be able to minimize the disagreement. Comprehensive data and analysis with multiple spacecraft (such as SDO, STEREO, SOHO, ACE, WIND, or other future missions) will probably help us develop the ability of including physically realistic coronal heating modules into 3D MHD codes, improve the determination of the structure of the ambient solar wind, and further numerically characterize the 3D propagation of CMEs through the heliosphere, as mentioned by Feng et al. (2010).

4. Summary

In this study, we use the 3D COIN-TVD MHD model and the magnetized plasma blob CME model to analyze the 2001 March 31 two-CMEs propagation and interaction event observed by SOHO/ACE. The dynamical propagation and interaction of the two CMEs between 2.5 and 220 Rs are investigated. Our simulation results show that, the second CME can overtake the first one, and cause compound interactions and an obvious acceleration of the shock as shown in Fig. 3. By looking at our simulation results including Fig. 4, we find that at L1 point near the Earth, the two resultant magnetic clouds in our simulation are consistent with the observations by ACE. While there still exist limitations in our model, which we will hope to overcome in our future investigation.

Acknowledgments. The work performed by F. Shen and X. Feng is supported by National Natural Science Foundation of China (41174150, 41031066, 41074121 and 40921063), 973 key project 2012CB825601, the Specialized Research Fund for State Key Laboratories and the Public science and technology research funds projects of ocean (201005017). S. T. Wu is supported by AFOSR grant number FA9550-07-1-0468, NSF grant number ATM-0754378 and NSO/AURA grant number C-10569A which is a subaward of NSF Award No. 0132798.

References

Burlaga, L. F., Plunkett, S. P., & St. Cyr, O. C. 2002, J. Geophys. Res., 107(A10), SSH 1-1
Chané, E., C. Jacobs, B. Van der Holst, S. Poedts, & D. Kimpe 2005, A&A, 432, 331
Chané, E., B. Van der Holst, C. Jacobs, S. Poedts & D. Kimpe 2006. A&A, 447, 727
Chané, E., S. Poedts & B. Van der Holst 2008, A&A, 492, L29
Feng, X., et al. 2005 Chin. Sci. Bull., 50(7), 672
Feng, X., Yang, L. P., Xiang, C. Q., et al. 2010, ApJ, 723, 300
Lugaz, N., Manchester, W. B., IV, & Gombosi, T. I. 2005, ApJ, 634(1), 651
Lugaz, N., & Roussev, I. I. 2011, JASTP, 73(10), 1187
Shen, F., Feng, X., Wu, S. T.,& Xiang, C. 2007, J. Geophys. Res., 112, A06109
Shen, F., Feng, X.& Song, W. B. 2009, Sci. in China, 52(10), 2895
Shen, F., Feng, X., Xiang, C., & Song, W. B. 2010, JASTP, 72(13), 1008
Shen, F., Feng, X., Wu, S. T. Xiang, C., & Song, W. B. 2011, J. Geophys. Res., 116, A04102
Shen, F., Feng, X., Wang Y., Wu, S. T., et al. 2011. J. Geophys. Res., 116, A09103
Tóth, G. 2000, J. Comput. Phys., 161, 605
Wang, Y. M., Ye, P. Z. & Wang, S. 2003, J. Geophys. Res., 108, 1370
Wang, Y., Zheng, H., Wang, S., & Ye, P. 2005, A&A, 434, 309
Wei, F. S., Feng, X. S., Cai, H. C., & Zhou, Q. J. 2003. J. Geophys. Res., 108(A6), 1238
Wu, S. T. & Wang, J. F. 1987, Comp. Meth. Appl. Mech. Engg., 64, 267
Wu, S. T., Guo, W. P., Michels, D. J., & Burlaga, L. F. 1999, J. Geophys. Res., 104(A7), 14789
Wu, S. T., Wang, A. H., Liu, Y., & Hoeksema, J. T. 2006, ApJ, 652, 800